Identification of carbonaceous deposits formed on H-mordenite during alkane isomerization

Matthew J. Wulfers and Friederike C. Jentoft [*]

School of Chemical, Biological & Materials Engineering, University of Oklahoma, Norman, OK 73019-1004, USA; *corresponding author: fcjentoft@ou.edu

Abstract

To identify hydrocarbon surface species accumulating during alkane isomerization, a strategy involving in situ UV–vis and FTIR spectroscopies, reaction of formed species with various bases, adsorption of reference compounds, and extraction of spent catalysts was applied. During conversion of *n*-butane or *n*-pentane on H-mordenite at reaction temperatures below ≈ 550 K, species characterized by an intense absorption band at a wavelength of 292–296 nm were observed by in situ diffuse reflectance UV–vis spectroscopy. Species with a comparable electronic signature formed after adsorption of 1-butene, 1-pentene, or 1-hexene, indicating that olefins are intermediates in the formation of carbonaceous deposits from alkanes. The chromophore was largely invariant to the carbon chain length and the species were identified as alkyl-substituted cyclopentenyl cations. Carbonaceous deposits formed at temperatures higher than ≈ 550 K consisted of methyl-substituted naphthalenes, anthracenes, and tetracenes; these species also existed as stable cations on the zeolite during catalysis, producing a broad absorption at 350–500 nm. The polycyclic aromatic species were neutralized by water vapor, whereas the alkyl-substituted cyclopentenyl cations required a stronger base, such as ammonia.

Keywords: carbonaceous deposits; coke; skeletal isomerization; paraffins; alkenes; *solid acid*; allylic; monoenylic; cyclopentenyl; acenes; gas phase basicity; deactivation

1. Introduction

Skeletal isomerization of *n*-alkanes is an important process in petroleum refining. Conversion of *n*-pentane and *n*-hexane to their skeletal isomers is motivated by the increased octane number of the resulting product stream. An H-form zeolite, usually H-mordenite containing platinum, is used as the catalyst [1,2]. Isobutane is the product of *n*-butane skeletal isomerization and is needed for alkylation. The corresponding olefin, isobutene, is needed for production of methyl and ethyl *tert*-butyl ethers (MTBE and ETBE). Conversion of *n*-butane to isobutane is usually performed using a platinum-containing chlorided alumina catalyst [3].

The combination of platinum in the catalyst and H_2 in the feed is used to prevent buildup of carbonaceous deposits. As platinum is expensive and H_2 availability is limited, a catalyst that could perform the skeletal isomerization at a stable rate without platinum and H_2 would be valuable. Design of such a catalyst may only be possible through a better understanding of the surface chemistry leading to both selective formation of the desired products and formation of carbonaceous deposits. The goal of this contribution is to identify the irreversibly adsorbed species that form on H-mordenite during alkane conversion.

Methods for analysis of carbonaceous deposits can be divided into two broad categories: i) ex situ (post-mortem) and ii) in situ. The main deficiencies of ex situ methods are that they may not deliver information on the deposits as they exist during catalysis and that they often require additional chemical treatments before analysis. Guisnet and co-workers [4] developed a procedure involving digestion of spent zeolites in hydrofluoric acid, liquid–liquid extraction with dichloromethane, and GC-MS or HPLC analysis of the dichloromethane extract, that can be used for speciation of some organic residues. Only species that will partition into the organic phase can be detected by this method, which has led to the frequently made distinction between

"soluble" coke containing olefinic, naphthenic, and smaller aromatic compounds, and "insoluble" coke generally consisting of polycyclic aromatic hydrocarbons [5,6]. Although the inventors did extensive tests to exclude that coke is altered during the extraction process, doubts have occasionally been voiced [7]. In any case, post-mortem analysis does not deliver information about a possible charged state of surface deposits. Indeed, in situ analysis has shown that some aromatic species exist as cations on the working catalyst [8,9]. A recent review of coke characterization techniques, including several that are performed ex situ, has been provided by Bauer and Karge [10].

In situ methods can deliver information about the deposits as they exist on the working catalyst. For example, discrimination between the neutral or cationic state of a species is possible. In situ diffuse reflectance spectroscopy can be performed, with the proper equipment, under flow conditions at elevated temperatures, allowing for the active catalyst to be monitored. UV-vis spectroscopy is particularly sensitive to the $\pi \rightarrow \pi^*$ transitions of unsaturated hydrocarbons, which often account for a significant portion of the carbonaceous deposits. Infrared spectroscopy can also be performed under working conditions, but the absorption coefficients of vibrational transitions are usually orders of magnitude smaller than those of electronic transitions [11]. Another advantage of UV-vis spectroscopy is the absence of strong absorptions from the zeolite in the wavelength range of interest. In contrast, the intense vibrational bands of the zeolite lattice and absorption bands by the gas phase reactant in diffuse reflectance IR spectra can make identification of vibrations from the carbonaceous deposits difficult.

In situ UV-vis spectroscopy has previously been used for the purpose of identifying organic residues formed during conversion of methanol [8,9,12,13], ethene [14], *n*-butane [15-

18], and *n*-pentane [17,19]. Interpretation of bands formed during catalysis often relies on comparison with spectra of adsorbed reference compounds. Infrared spectroscopy can be used to provide complementary information. A strategy involving both UV–vis and IR spectroscopies to identify surface species formed on solid acids has been used in the past [20-27]. Band assignments can be retrieved from the review by Bauer and Karge [10].

Deactivation and coke formation during alkane isomerization on H-mordenite have been associated with high olefin levels in the feed [28,29], and it has been demonstrated that surface reaction products from 1-butene are similar to those formed during butane conversion [15]. The role of olefins for the formation of carbonaceous deposits in general has been emphasized in various reviews [6,30].

In this contribution, in situ diffuse reflectance UV–vis–NIR and infrared spectroscopies, and extractions of spent catalysts, are used to investigate the carbonaceous deposits formed during conversion of alkanes on H-mordenite, a well-characterized solid acid [31,32]. Two reactants, *n*-butane and *n*-pentane, are used to demonstrate that the important characteristics of surface deposits are independent of the carbon chain length and are rather a function of reaction temperature. Olefins are the intermediates between alkanes and surface deposits and lead to the same characteristic species as alkanes. The indifference of the deposit characteristics to reactant chain length is also seen during adsorption and reaction of 1-butene, 1-pentene, and 1-hexene. Surface species can be transformed from a cationic to a neutral state through reaction with base, and the availability of spectra of both states is found to be essential for species identification. By using reagents with varying base strength, specifically water and ammonia, the basicity of the carbonaceous deposits can be estimated and used as additional piece of information. In addition

to analyzing the carbonaceous deposits formed in this specific scenario, an effective strategy for identification and characterization of organic surface species is presented.

2. Materials and Methods

2.1 Materials

Mordenite was provided by UOP. One sample (Lot #32125-99) was received as NH_4-mordenite and had a Si/Al ratio of 9.1 specified by ICP-AES. Another sample (Sample ID AS33805-74B) was received as Na-mordenite and had a Si/Al ratio of 5.4. This sample was ion-exchanged with 1 M NH_4NO_3 for 6 h at 333 K. Calcination was performed at a temperature of 823−873 K in a flow of synthetic air. The calcined H-forms of these materials will be referred to as M1 (Si/Al = 9.1) and M2 (Si/Al = 5.4).

Gases were of the following purities: *n*-butane (Matheson, 99.99%) containing 14 ppm isobutane and < 1 ppm propene impurities, 1-butene (Sigma, ≥ 99%), 2% ammonia in helium (Airgas), N_2 (Airgas, UHP 99.99%), O_2 (Airgas, UHP 99.994%), H_2 (Airgas, UHP 99.999%), and helium (Airgas, UHP 99.999%). N_2, O_2, H_2, and helium were passed through moisture traps (Agilent, MT400-2 for N_2, O_2, and H_2; Restek for helium), and N_2 was additionally passed through an O_2 trap (Chromres, Model 1000). Liquids were: *n*-pentane (Sigma, ≥ 99%), 1-pentene (Sigma, 98%), and 1-hexene (Sigma, 99%).

2.2 Spectroscopic equipment

A Lambda 950 spectrometer (PerkinElmer) was used to perform UV−vis−NIR spectroscopy. The diffuse reflectance experiments were performed using a Praying Mantis™ diffuse reflectance accessory (DRP-P72, Harrick Scientific). The in situ experiments were conducted in an HVC-VUV environmental chamber (Harrick Scientific). Fluorilon-99 (Avian

Technologies) served as a diffuse reflectance standard; the background was recorded with a disk of this material placed in the environmental chamber.

In situ Diffuse Reflectance Infrared Fourier Transform Spectroscopy (DRIFTS) was performed with a Spectrum 100 spectrometer (PerkinElmer). A Praying Mantis™ diffuse reflectance accessory (DRP-P11, Harrick Scientific) was used with a CHC-CHA-3 environmental chamber (Harrick Scientific). Potassium bromide (Sigma, FT-IR grade) was dried in situ and used to record the background spectrum. KBr was also used to dilute the zeolites in some measurements.

2.3 *n*-Butane and *n*-pentane conversion with in situ spectroscopic analysis

Conversion of *n*-butane or *n*-pentane was performed in the environmental chambers described in Section 2.2. Effluent gases were analyzed using a Varian 3800 GC equipped with a Fused Silica PLOT (Chrompack, 0.32 mm ID x 60 m) column and a flame ionization detector. Before reaction, the zeolite (M1) was pre-treated by heating to a temperature of 773 K for a series of 0.5 h treatments in flowing synthetic air, N_2, and H_2. The chamber was then cooled to reaction temperature. The reported temperature is the set point of the chamber.

Conversion of both *n*-butane and *n*-pentane occurred at atmospheric pressure. For *n*-butane, the total gas flow rate was 30 ml min^{-1} (NTP) with an *n*-butane partial pressure of 10 kPa and a balance of either H_2 or helium. For *n*-pentane, the total gas flow rate was 34 ml min^{-1} with an *n*-pentane partial pressure of 13 kPa and a balance of helium. The *n*-butane and *n*-pentane weight hourly space velocities (W/F) were 0.16 h and 0.08 h, respectively. Except for *n*-pentane, gas flow rates were controlled using mass flow controllers. To add *n*-pentane to the gas stream, helium was passed through liquid *n*-pentane in a three-legged saturator. The saturator was held at 257 K by placing it in a temperature-controlled bath of ethylene glycol and water. Gas lines were heated to 353 K.

2.4 In situ spectroscopic analysis of adsorption and reaction of olefins

H-mordenite was dried at temperatures of 573 to 673 K in the in situ cell and then cooled to the desired adsorption temperature in inert gas. Details of the pre-treatments and heat treatments following adsorption are provided in the figure captions. The olefin (in the case of 1-pentene or 1-hexene liquid or vapor as specified) was injected with a syringe into the gas stream through a septum; liquids vaporized in the heated lines and reached the sample as a vapor. For experiments in which H_2O vapor was applied, the inlet gas stream was diverted through a saturator containing liquid water.

2.5 Adsorption of olefins with subsequent digestion and extraction

Two hundred fifty milligrams of H-mordenite (M2) powder was loaded into a 12 mm ID tubular reactor made from quartz and equipped with a quartz frit to support the catalyst bed. The reactor was placed in a vertical furnace. For pre-treatment, the sample was heated to 673 K while flowing 50 ml min^{-1} of synthetic air, held at 673 K for 1 h also in air flow, and then cooled to 323 K in 50 ml min^{-1} of N_2.

1-Butene was then admitted to the gas stream via mass flow controller in the amount of 45 μmol. The furnace then either remained at 323 K for 1 h or was heated after 5 minutes to 573 K and held at this temperature for 1 h. The zeolite powder was then removed from the reactor and a diffuse reflectance UV–vis spectrum was taken. During the transfer and the acquisition of the UV–vis spectrum, the zeolite was exposed to ambient conditions.

The zeolite was then placed in a polyethylene vial and aqueous hydrofluoric acid (Mallinckrodt, 49%) was added in the ratio of 8 ml g^{-1} zeolite. After 30 minutes, 4 ml of dichloromethane (Macron, 99.5%) was added. The liquid–liquid extraction was allowed to occur overnight. The dichloromethane phase was transferred to a different polyethylene vial and neutralized with a 0.01 M calcium hydroxide (Sigma, 95+%) solution. Species in the

dichloromethane extract were then analyzed with a GC-MS (Agilent 5975E) using an HP-5MS column (Agilent, 0.25 mm ID x 30 m) for separation.

3. Results

3.1 *n*-Butane conversion on H-mordenite: Catalytic performance and in situ spectroscopy

When H_2 was used as the diluent, the performance was stable (Fig. 1, first 1.5 h), and no bands formed in the UV−vis spectra (Fig. 2). Isobutane, propane, and pentanes were the main products. The formation rates at 563 K in the in situ cell were somewhat lower than expected from experiments performed in an isothermal packed bed reactor. To a large extent, this discrepancy can be explained by a temperature gradient in the catalyst bed caused by the heater placement. When H_2 was replaced with helium (Fig. 1, after 1.5 h), product formation rates increased by a factor of 20 and then slowly decreased with time on stream. With H_2 as the diluent, the only olefins detected in the effluent were *n*-butenes at a concentration of 4 ppm. After changing the diluent to helium, the concentration of *n*-butenes immediately increased to 14 ppm and then decreased. Concurrent with the slow deactivation was the growth of a band at a wavelength of 286−292 nm. The absorption maximum of this band was initially at 286 nm and then slowly shifted to 292 nm with time. The Kubelka−Munk value at 292 nm is plotted versus time on stream in Fig. 1. Bands with less intensity relative to the 292 nm band were formed at longer wavelengths; a shoulder around 335 nm, a distinct band at 395 nm, and a broader band around 455 nm were noted. The UV−vis spectra of the deposits formed at 563 K are markedly different than the spectra of the deposits formed at 623 K [15] in that the bands at longer wavelengths are much less developed.

During conversion of *n*-butane at 563 K using helium as a diluent, only very weak bands evolved in the IR spectra. However, during conversion at 633 K, a well resolved band between

wavenumbers of 1580–1620 cm^{-1} grew with time on stream, as shown in Fig. 3. The band was initially centered at 1605 cm^{-1}; with time the position of maximum absorbance shifted to 1596 cm^{-1}. These IR spectra collected at a temperature of 633 K can be associated with UV–vis spectra collected under comparable conditions [15].

3.2 *n*-Pentane conversion on H-mordenite: Catalytic performance and in situ UV–vis spectroscopy

During conversion of *n*-pentane with helium as a diluent, product formation rates decreased with time on stream as shown in Fig. 4. Isobutane was the main product at 3 minutes on stream but 2-methylbutane was the main product at every point thereafter. Propane, *n*-butane, and hexanes (*n*-hexane, 2-methylpentane, 3-methylpentane, and 2,2-dimethylbutane) were also formed.

Concurrent with the decrease in catalytic performance was the growth of a band in the UV range at a wavelength of 293–295 nm as shown in Fig. 5. The absorption maximum was at 293 nm after 10 minutes on stream and shifted to 295 nm with time. The Kubelka–Munk value at 295 nm is plotted versus time on stream in Fig. 4.

3.3 Spectra collected in situ at temperatures below ≈ 550 K after adsorption of 1-butene, 1-pentene, or 1-hexene

The electronic bands that formed after adsorption of 1-butene, 1-pentene, and 1-hexene were all similar. After 1-pentene was adsorbed at 303 K, bands initially formed at wavelengths of 205 and 320 nm (Fig. 6). With time, the band at 320 nm decreased in intensity while a new band with a maximum absorption between 295 and 300 nm grew. An isosbestic point at 314 nm was evident. As the catalyst was heated, the new band became symmetric and well-defined, with a maximum absorption at 295 nm. A smaller band at 215 nm also grew. A band at 385 nm grew initially and then shrunk. The most intense band formed after 1-butene adsorption at a

temperature of 443 K was at 296 nm and has been reported previously [15]. The most intense band formed after 1-hexene adsorption was at 295 nm (Fig. S1).

The introduction of water vapor, which is known to neutralize some cationic species on solid acids [33], had a minimal effect on the 295 nm band produced through 1-pentene adsorption. When water vapor was admitted, the band slowly decreased in intensity while new bands formed at 372 and 456 nm (Fig. S2). Ammonia had a much different and more immediate effect; the main band was completely eroded and a new band formed at 255 nm (Fig. 7). In the absence of basic reagents in the gas flow the cationic species was stable, as evident by the near constant band intensity 1 h after admission of 1-pentene (Fig. 7). During admission of ammonia, no hydrocarbon fragments were observed in mass spectra recorded of the reactor effluent.

Adsorption of 1-pentene at 453 K (the same temperature at which the conversion of *n*-pentane was performed) resulted in formation of bands in the infrared range at 2970, 2935, 2905, 1505 and 1400–1350 cm^{-1} (Fig. 8). The intensity of the band of the bridging OH groups at 3604 cm^{-1} decreased without concomitant formation of a band at lower frequency that would indicate mere perturbation of the OH groups. The intensity of the bands at 1610–1650 and 1875 cm^{-1} also decreased.

3.4 Evolution of UV–vis spectra during heating and subsequent exposure of the sample to water vapor

Independent of how they were formed, the surface species characterized by the band at 292–296 nm reacted in the same way. When H-mordenite samples with these surface species were heated to ≈ 573 K or above, the band at 292–296 nm was partially consumed while new bands formed at wavelengths longer than 350 nm. Spectra demonstrating this behavior have been reported previously [15]. The new bands at longer wavelengths were eroded when the sample

was exposed to water vapor, as shown in Fig. 9. In this experiment, *n*-butane conversion was performed on H-mordenite at 636 K for 2 h using helium as the diluent and the reaction chamber was cooled to room temperature while a helium flow was maintained through the catalyst bed. When water vapor was then added to the gas stream, the intense bands at 395 and 460 nm were replaced by many new, less intense bands between 350 and 500 nm, and two new bands with Lorentzian shape appeared below 300 nm. The effect of water was largely reversible; that is, the broad bands at 395 and 460 nm were almost completely recovered when the humidified zeolite was re-heated (Fig. S3).

3.5 Extraction of deposits formed on H-mordenite

Extraction of the solubilized H-mordenite that had been exposed to either 1-butene or 1-pentene at 323 K revealed a mixture of aliphatic hydrocarbons with a broad distribution of molecular weights. The hydrocarbons contained a number of carbon atoms not necessarily corresponding to multiples of 4 or 5 (*viz.*, the number of carbon atoms in the reactants). Alkanes and species with one double bond were detected in the mixture. A GC-MS chromatogram of the dichloromethane extract from H-mordenite exposed to 1-butene at 323 K is shown in the Supporting Information (Fig. S4). The extract from H-mordenite exposed to 1-pentene gave a similar chromatogram. The UV–vis spectrum of the H-mordenite before digestion showed a band at 295 nm, whereas the spectrum of the dichloromethane extract did not (Fig. S5). Consistently, the GC-MS analysis did not lead to identification of a structural unit in the extract that would give rise to absorption close to 295 nm.

To be able to assign the bands observed at wavelengths > 350 nm, additional information was gathered. 1-Butene was adsorbed on H-mordenite, heated to 573 K in a tubular packed bed reactor, and the zeolite was then digested and extracted. The extract contained alkyl-substituted naphthalene and anthracene species (Fig. S6). The naphthalenes contained up to four methyl

groups and the anthracenes contained up to three methyl groups. The concentration of naphthalenes was in the order of methylnaphthalene > dimethylnaphthalene > trimethylnaphthalene > tetramethylnaphthalene > naphthalene. The concentration of anthracenes was in the order of dimethylanthracene > trimethylanthracene > methylanthracene.

The UV–vis spectrum of the H-mordenite that was reacted with 1-butene in the tubular reactor and then exposed to ambient air (Fig. 10) was similar to the spectrum of the catalyst that was used for conversion of *n*-butane at 636 K and then exposed to water vapor in the in situ cell (Fig. 9). The spectrum of the dichloromethane extract contained many of the same bands seen in the spectrum of the zeolite before digestion (Fig. 10). Both on the solid zeolite and in the dichloromethane extract, bands with Lorentzian character were present at 228 nm and 257 nm. The bands positions at wavelengths > 320 nm were similar, and the bands were less intense than the shorter wavelength bands. A band with Lorentzian character at 278 nm and a shoulder at 300 nm existed on the zeolite but were not distinctly resolved in the dichloromethane extract.

4. Discussion

4.1 Overview

An overview of the experiments is given in Fig. 11. Conditions had to be adjusted to the reactivity of the reactants; catalysis using alkanes as reactants required higher temperatures than conversion of olefins, all of which were very reactive already at room temperature. The surface chemistry and the stable surface species that were observed depended more on the reaction temperature than on the reactant. After comparing the catalytic data with literature reports, the discussion thus follows the evolution of surface species with increasing temperature.

4.2 Catalytic performance of H-mordenite in *n*-butane and *n*-pentane conversion

The main products formed during *n*-butane conversion are consistent with those in earlier reports [34,35]. Isobutane was the main product and propane and pentanes (*n*-pentane and 2-methylbutane) were the most abundant side products. We previously reported that H_2 has a stabilizing effect on the performance of H-mordenite in the conversion of *n*-butane at 623 K and elaborated on the possible reasons [15]. A similar stabilizing effect of H_2 was observed in this work, with the catalysis performed at a lower temperature (563 K). When H_2 was replaced by helium, unsaturated deposits accumulated on the catalyst surface [15 and this work] and the rate of product formation first increased dramatically and then declined. These effects are ascribed to higher concentrations of butenes in absence of H_2, which are known to both promote deactivation [28,29,36] and increase the rate of alkane conversion [28,37]. Higher concentrations of butenes were measured, 14 ppm immediately after switching to helium vs. 4 ppm in H_2. The deactivation is in discord with observations made by Engelhardt [37], who found H-mordenite, even without H_2 in the feed, to be capable of stable operation during *n*-butane conversion. Olefin levels in the effluent stream seem comparable to those measured here, making it more likely that variations among zeolite samples are responsible for the different deactivation behavior. In any case, the role of H_2 is obviously to control the butene concentration.

The performance of H-mordenite in the conversion of *n*-pentane was also as expected. The bare zeolite is known to deactivate rapidly in the absence of a noble metal and H_2 [38]. Essayem et al. [39] operated with similar reaction conditions to those used in this work and found H-mordenite to lose 80% of its activity after 1 h. They also observed that isobutane was produced with the highest initial rate, but 2-methylbutane became the main product after 1 h. In this work, isobutane was also the main product at 3 minutes on stream, and 2-methylbutane was the main product at every point thereafter. The decrease in conversion over 2 h was 75%.

4.3 Identification of species formed at temperatures below ≈ 550 K

A well-defined, symmetric band at 292–296 nm emerged in the spectra of H-mordenite recorded during *n*-butane conversion, during *n*-pentane conversion, and during gentle heating after adsorption of 1-butene, 1-pentene, or 1-hexene. Thus, the discussion and interpretation of this band apply to all of these scenarios. Bands formed after adsorption of aliphatic hydrocarbons on solid acids in this region of the UV–vis spectrum are typically assigned to monoenylic cations [20,40-43], which are simple allylic cations without further conjugation that can form through protonation of a diene or hydride abstraction from a monoene. Melsheimer et al. [14] assigned a band at 280–310 nm on HZSM-5 formed from ethene to cyclopentenyl and cyclohexenyl species. Cycloalkenyl cations were also named by Knözinger [44] as a possible assignment for a band at 292 nm that formed during *n*-butane conversion on sulfated zirconia.

The assignment of electronic bands arising from hydrocarbons adsorbed on solid acids relies strongly on comparison with the spectra of species prepared in solution, where the chemistry can be more carefully controlled. For monoenylic cations, Sorensen et al. [45] found the cation formed by protonation of 2,4-dimethyl-1,3-pentadiene in sulfuric acid to absorb at 305 nm, and Deno et al. [46] found the 2,4-dimethylpentenyl and 2,3,4-trimethylpentenyl cations to absorb at 305 nm and 307 nm, respectively. Deno et al. [46] also found the position of the monoenylic species formed by protonation of a variety of alkyl-substituted cyclopentadienes to vary with the type and position of alkyl substituents. For example, 1,3-dimethylcyclopentenyl absorbed at 275 nm, 1-ethyl-3-methylcyclopentenyl absorbed at 278 nm, and 1,2,3,4,4,5-hexamethylcyclopentenyl absorbed at 301 nm. Thus, in solution, the longest reported wavelength for a methyl-substituted cyclopentenyl species is 301 nm, implying that most of this type of cyclic species absorb below 300 nm, whereas the absorption of acyclic methyl-substituted pentenyl species is observed at wavelengths longer than 300 nm.

Assignment of the 292–296 nm band to a monoenylic cation is supported by the intense band at 1505 cm^{-1} that formed after adsorption of 1-pentene (Fig. 8). Bands in this region of the infrared spectrum are characteristic of carbon–carbon bonds with an intermediate bond order between 1 and 2, and are often attributed to monoenylic cations. In solution, the infrared spectrum of a symmetrically substituted allyl cation has a sharp absorption at 1530 cm^{-1} [47]. Bands at similar positions have been found after adsorption of olefins on solid acids. After adsorption of propene on HZSM-5, a band formed at 1510 cm^{-1} and was assigned to an allyl carbenium ion [20]. Bands at 1490–1530 cm^{-1} were formed after adsorption of numerous cyclic olefins on H-form zeolites and were assigned to alkenyl carbenium ions [26]. Pazè at al. [25] found bands at 1500 cm^{-1} and 285 nm after adsorption of 1-butene on H-ferrierite and heating to 473 K. The authors pointed out the general problem of distinguishing band shifts resulting from a charged state from those resulting from the presence of substituents. While the IR band was considered to not provide conclusive information, the UV band was assigned to neutral conjugated polyenes. However, for a neutral conjugated polyene to absorb at 285 nm, three to four double bonds are required, depending on the number of alkyl substituents [48]. The infrared band for C=C stretching vibrations in a highly conjugated acyclic species is typically around 1600 cm^{-1} [49]; for example, 1,3,5-hexatriene has a strong absorption at 1612–1623 cm^{-1} [50]. As both bands reported by Pazé et al. cannot be assigned to the same neutral polyene, they may alternatively be attributed to a monoenylic cation.

Formation of bands at 295 nm and 1505 cm^{-1} after adsorption of 1-pentene is consistent with formation of monoenylic cations. However, discriminating between the cyclic or acyclic nature of monoenylic species is difficult with only the UV–vis and infrared spectra of the cationic form of the species. Ammonia is commonly used to neutralize cations on solid acids

[22,33]. Here, it produced a species absorbing at 255 nm from that absorbing at 293 nm (Fig. 7). Monoenylic species should be converted to dienes through application of ammonia. The UV–vis spectrum of the neutral diene provides additional information that can potentially be used to discriminate between cyclic and acyclic species. Because the ring of a cyclic entity provides an additional degree of unsaturation, cyclic dienes absorb at longer wavelengths than acyclic dienes. For example, 1,3-butadiene absorbs UV radiation at a wavelength of 217 nm [48] and cyclopentadiene absorbs UV radiation at a wavelength of 240 nm [51]. As the Woodward–Fieser rules apply to conjugated dienes, addition of alkyl groups should cause a +5 nm shift per group [48]. Thus, eight alkyl groups would be required on the neutral species to explain the absorption band at 255 nm. Only three to four alkyl groups are required on cyclopentadiene to explain the same band. It has been reported that addition of basic reagents can facilitate desorption of carbonaceous deposits [52], which would also result in a decrease in band intensity. However, no hydrocarbons were detected in the effluent during application of ammonia. Thus, the effect of ammonia is to neutralize the alkyl-substituted cyclopentenyl species and not to cause them to desorb. Monoenylic cations have larger absorption coefficients than the corresponding neutral species [53], which explains the decline in integral intensity.

Formation of methyl-substituted cyclopentenyl species has been observed in numerous ^{13}C NMR investigations of adsorption and reaction of olefins on zeolites and the species are considered to be extremely stable. For example, Stepanov et al. [54] found 1,2,3-trimethylcyclopentenyl ions to be formed from 1-butene on H-ferrierite. Haw and co-workers found evidence that methyl-substituted cyclopentenyl species formed from propene on HY [55] and from ethene on HZSM-5 [56]. Methyl-substituted cyclopentadienes have a high gas phase proton affinity, making them excellent candidates to persist in zeolites as cations. For example,

Nicholas et al. [57] calculated the gas phase proton affinity of 1,3-dimethylcyclopentadiene to be 903 kJ mol^{-1}. Fang et al. [58] calculated the gas phase proton affinity of 1,2,3-trimethylcyclopentadiene to be 918 kJ mol^{-1} and found that the most energetically favored state for methyl-substituted cyclopentadienes adsorbed in several zeolites is the cationic state. Consumption of acidic OH groups (Fig. 8) indicates that proton transfer to a hydrocarbon species takes place at some point of olefin conversion. The obtained surface cations can be neutralized provided a sufficiently strong base is used. For example, the proton affinities of water, ammonia, and pyridine are 696, 853, and 930 kJ mol^{-1}, respectively [59]. These values apply for the free molecules and ions in the gas phase, and it is conceivable that the influence of the zeolitic surroundings makes possible the neutralization of alkyl-substituted cyclopentenyl species by ammonia. In light of the combined experimental evidence and information from the literature, the bands at 292–296 nm and 1505 cm^{-1} are assigned to alkyl-substituted cyclopentenyl species.

Additional confirmation of this assignment was sought through digestion and extraction of H-mordenite that had reacted with 1-butene or 1-pentene at 323 K. The extraction procedure was validated by the fact that the GC-MS data revealed a diverse mixture of paraffins and olefins of varying chain length. This result is consistent with the work of Guisnet and co-workers [4], who adsorbed propene on USHY at 393 K and found the extract to contain polymers with the number of carbon atoms not equal to multiples of three, olefins, and naphthenes. However, the UV–vis spectrum of the dichloromethane extract did not show a band at 295 nm (Fig. S5), suggesting that the species responsible for this absorption was either transformed or was not recovered. As the alkyl-substituted cyclopentadienes have high proton affinities, it is possible that the species remained protonated and stayed in the hydrofluoric acid during the liquid–liquid extraction with dichloromethane. Sorensen [45] used a combination of neutralization with

potassium hydroxide and extraction with hexane to recover protonated polyenes from sulfuric acid with less than 50% yields. It is also worth noting that digestion and extraction of used methanol-to-hydrocarbons catalysts has also not resulted in recovery of neutral forms of alkyl-substituted cyclopentenyl species [60-62], even though the ionic forms are known, or at least suspected, to be important intermediates for conversion of methanol-to-hydrocarbons on zeolite and zeotype catalysts [63-65]. While the extraction could not confirm the cycopentadiene-derived monoenylic species, the findings are explainable and do not contradict the interpretation.

For a monoenylic species to be formed from an olefin, abstraction of a hydride must occur. Thus, a Lewis acid is necessary. The Lewis acidity can be provided by either coordinatively unsaturated extraframework aluminum in the zeolite or from carbenium ions. Another pathway leading to formation of monoenylic species is protonation of a diene, however hydride abstraction is also a necessary step in the acid-catalyzed formation of a diene from a monoene. The band at 320 nm formed immediately after admission of 1-pentene (Fig. 6) could be representative of an initial acyclic monoenylic species formed either directly from 1-pentene or after oligomerization, deprotonation, and hydride abstraction. In order for a cyclic species to form, a 1,5 cyclization reaction must occur, requiring formation of an intermediate dienylic cation. Dienylic species absorb at longer wavelengths than monoenylic species; for example, Sorensen [45] reported that the dienylic species formed by protonation of 2,6-dimethyl-1,3,5-heptatriene absorbs at 396 nm. On zeolites, dienylic species have been reported to absorb between 350–380 nm [20]. In fact, a small band at 384 nm grew during heating and then shrunk (Fig. 6, inset). Thus, the band at 384 nm is assigned to an acyclic dienylic cation.

4.4 Identification of species formed at temperatures above ≈ 550 K

Bands formed at 350–500 nm after heating a zeolite containing species absorbing at 292–296 nm to temperatures greater than ≈ 550 K [15]. It is important to note that 550 K is an

estimate of the actual temperature at which the formation of bands at wavelengths longer than 350 nm begins to take place, because of the inaccuracy of the temperature measurement in the in situ cell and the low time resolution (about 10 min per spectrum).

There are four pieces of information regarding the identity of the deposits formed above ≈ 550 K. GC-MS and UV–vis analysis of the dichloromethane extract after digestion of the zeolite in hydrofluoric acid (Figs. S6 and 10) and the UV–vis spectrum of the catalyst after exposure to water vapor (Figs. 9 and 10) provide information on the neutral species. The in situ UV–vis and infrared spectra provide information on the species as they exist on the zeolite, probably as cations (Figs. 3 and 9, and [15]). The discussion of results will proceed in this order.

The GC-MS chromatogram of the extracted deposits revealed mostly naphthalenes and anthracenes, and a few non-chromophoric impurities leached from the polyethylene vials. The transition away from "low temperature coke" is said to occur around 473 K, with polyaromatic coke dominating at 623 K [6]. On H-mordenite, phenanthrene was identified at 613 K [5]. Polynuclear aromatics formed on H-mordenite from ethylene at and above 550 K [66]. Stepanov et al. [54] found polycyclic aromatics to form on H-ferrierite already at 523 K. Thus, the formation of polycyclic aromatics at ≈ 550 K is in agreement with previous reports.

The UV–vis spectra of the catalyst taken in situ after exposure to water vapor or ex situ (after exposure to atmospheric water vapor) are representative of the deposits in their neutral state. The neutralizing effect of water vapor has been reported previously by Leftin and Hobson [33] who used it to neutralize the trityl cation on silica–alumina. Subsequent analysis showed that water did not cause hydrolysis of the cationic species with formation of triphenylmethanol, but instead triphenylmethane was recovered. Likewise, no hydroxylated aromatics were found in the dichloromethane extract, confirming that neutralization occurs and not hydrolysis. According

to the GC-MS analysis, the most prevalent naphthalene was 2-methylnaphthalene, which has a band with partial Lorentzian shape at 224 nm ("E" band) and a broader benzenoid band ("B" band) characterized by a fine structure with maxima at 266, 275, and 286 nm [67]. The most prevalent anthracenes had two methyl groups but the location of these groups could not be determined exactly. A representative example would be 1,3-dimethylanthracene which has an E band at 257 nm and a B band characterized by fine structure bands at 343, 360, and 380 nm [68]. Thus, the band at 228 nm in Fig. 10 is assigned to methyl-substituted naphthalenes and the band at 257 nm is assigned to methyl-substituted anthracenes. In the UV–vis spectrum the extract, the band at 228 nm is partially cut off through the absorption of the dichloromethane solvent in the UV range. The bands at 344, 359, and 381 nm are part of the fine structure of the anthracene B band. The bands at 447 and 473 nm in the spectrum of the solid zeolite are consistent with a methyl-substituted tetracene; tetracene has an intense E band at 278 nm and the most intense components of the B band are at 443 and 473 nm [69]. Tetracenes could not be detected in the extract, but they are known to have limited solubility in dichloromethane [70]. It is notable that the aromatic deposits are all members of the acene family, which suggests that the one-dimensional pore structure of H-mordenite plays a prominent role in determining the type of species that can form.

During conversion of alkanes, or after heating the initial surface products of olefin adsorption in the presence of inert gas, the polycyclic aromatic species exist in the zeolite as cations. The bands in the UV–vis spectra that were recorded in situ can be grouped into three main ranges of absorption, < 250 nm, 250–310 nm, and 370–500 nm. The bands at the longest wavelengths are central to the interpretation, because these bands can only be explained by neutral chromophores of a size and type that are unlikely to form under these conditions and for

which no other evidence exists, or by the cationic forms of the aromatic species detected in the extract. The assignment of these bands to the cations of acenes is consistent with the observation of the "coke band" in the IR spectra at 1580–1620 cm^{-1}, which is generally attributed to polycyclic aromatic species. Thus, on the working catalyst, the deposits exist as cations, indicating that they reside in the micropores of the zeolite.

Specific band assignments become possible through comparison of the spectra of the surface cations with the reported spectra of cations in mineral acids, specifically cations of the species identified in the extract by GC-MS. This comparison is straightforward because the band positions of aromatic cations have been shown to not vary significantly (± 5 nm) with the environment. For example, the UV–vis spectra of hexamethylbenzene [22] and anthracene [71] cations on a solid acid are very similar to the spectra of the same cations in a mineral acid [72,73]. In the series of naphthalene, anthracene, and tetracene cations, the wavelength of maximum absorption increases with the number of aromatic rings. The cations have been reported to absorb at 391, 408, and 447 nm, respectively [73]. Addition of methyl groups causes a modest shift in the wavelength of maximum absorption. For example, the strongest absorption bands of 1,4-dimethylnaphthalene and 2,3-dimethylnaphthalene cations undergo a 5–10 nm hypsochromic shift and that of the 2-methylanthracene [74] cation undergoes an even smaller bathochromic shift. Thus, the assignment of the electronic absorption bands at wavelengths larger than 380 nm to the cations of methyl-substituted naphthalene, anthracene, and tetracene is supported by the positions of the maximum absorptions of these cations in mineral acids.

5. Summary

Carbonaceous deposits formed on H-mordenite during conversion of *n*-butane or *n*-pentane originate from olefins. Below a reaction temperature of ≈ 550 K, a major fraction of

what may be referred to as “soft coke” was found to consist of alkyl-substituted cyclopentenyl cations, with characteristic absorptions at 292–296 nm and 1505 cm^{-1}. These species were neutralized through addition of ammonia, but not through addition of water vapor. Neutral alkyl-substituted cyclopentadienes species were not recovered by digestion of the zeolite in hydrofluoric acid and extraction with dichloromethane. At higher temperatures, the alkyl-substituted cyclopentenyl species reacted to form methyl-substituted naphthalenes, anthracenes, and tetracenes. Methyl-substituted naphthalenes and anthracenes were identified on the surface as well as by GC-MS and UV–vis spectroscopic analysis after digestion and extraction, whereas methyl-substituted tetracene was identified only on the surface and only by UV–vis spectroscopy. The aromatic species reside in the micropores of the zeolite and exist in their cationic form during catalysis. Upon admission of water vapor, the aromatic cations were neutralized.

6. Acknowledgements

The authors thank UOP LLC, a Honeywell company, for kindly providing the zeolite samples. The authors also thank A. Aho and D. Yu. Murzin for sharing their zeolite extraction procedure. This work was, in part, supported by the NSF EPSCoR award EPS 0814361.

7. References

[1] A.P.G. Kieboom, J.A. Moulijn, R.A. Sheldon, P.W.N.M. van Leeuwen, in R.A. van Santen, P.W.N.M van Leeuwen, J.A. Moulijn, B.A. Averill (Eds.), Catalysis: An Integrated Approach, Second, Revised, and Enlarged Ed., Elsevier, Amsterdam, 1999, v. 123, p. 39.
[2] P.M.M. Blauwhoff, J.W. Gosselink, E.P. Kieffer, S.T. Sie, W.H.J. Stork, in: J. Weitkamp, L. Puppe (Eds.), Catalysis and Zeolites: Fundamentals and Applications, Springer-Verlag, Berlin, 1999, p. 491.
[3] P.R. Robinson, in: C.S. Hsu, P.R. Robinson (Eds.), Practical Advances in Petroleum Processing, Springer, New York, 2006, vol. 1, p. 41.
[4] P. Magnoux, P. Roger, C. Canaff, V. Fouche, N.S. Gnep, M. Guisnet, in: Studies in Surface Science and Catalysis – Catalyst Deactivation, Proceedings of the 4th International Symposium, vol. 34, Elsevier B.V., 1987, p. 317-330.

[5] M. Guisnet, P. Magnoux, Appl. Catal. 54 (1989) 1.
[6] M. Guisnet, P. Magnoux, Appl. Catal. A 212 (2001) 83.
[7] H. Fu, W. Song, J.F. Haw, Catal. Lett. 76 (2001) 89.
[8] W. Dai, M. Scheibe, N. Guan, L. Li, M. Hunger, ChemCatChem 3 (2011) 1130.
[9] L. Palumbo, F. Bonino, P. Beato, M. Bjørgen, A. Zecchina, S. Bordiga, J. Phys. Chem. C 112 (2008) 9710.
[10] F. Bauer, H.G. Karge, in: H.G. Karge, J. Weitkamp (Eds.), Characterization II, Springer-Verlag, Berlin Heidelberg, 2007, p. 249.
[11] W. Schmidt, Optical Spectroscopy in Chemistry and Life Sciences, Wiley-VCH, Weinheim (Germany), 2005.
[12] W. Dai, X. Wang, G. Wu, L. Li, N. Guan, M. Hunger, ChemCatChem 4 (2012) 1428.
[13] Y. Jiang, J. Huang, V.R. Reddy Merthala, Y.S. Ooi, J. Weitkamp, M. Hunger, Microporous Mesoporous Mater. 105 (2007) 132.
[14] J. Melsheimer, D. Ziegler, J. Chem. Soc. Faraday. Trans 88 (1992) 2101.
[15] M.J. Wulfers, G. Tzolova-Müller, J.I. Villegas, D.Y. Murzin, F.C. Jentoft, J. Catal. 296 (2012) 132.
[16] D. Spielbauer, G.A.H. Mekhemer, E. Bosch, H. Knözinger, Catal. Lett. 36 (1996) 59.
[17] R. Ahmad, J. Melsheimer, F.C. Jentoft, R. Schlögl, J. Catal. 218 (2003) 365.
[18] F.C. Jentoft, in: M. Che, J.C. Védrine (Eds.), Characterization of Solid Materials and Heterogeneous Catalysts: From Structure to Surface Reactivity, vol. 1&2, Wiley-VCH, 2012, p. 138.
[19] S. Kuba, P. Lukinskas, F.C. Jentoft, R.K. Grasselli, B.C. Gates, H. Knözinger, J. Catal. 219 (2003) 376.
[20] A.V. Demidov, A.A. Davydov, Mater. Chem. Phys. 39 (1994) 13.
[21] S. Bordiga, G. Ricchiardi, G. Spoto, D. Scarano, L. Carnelli, A. Zecchina, J. Chem. Soc. Faraday Trans. 89 (1993) 1843.
[22] M. Bjørgen, F. Bonino, S. Kolboe, K.-P. Lillerud, A. Zecchina, S. Bordiga, J. Am. Chem. Soc. 125 (2003) 15863.
[23] C. Flego, I. Kiricsi, W.O. Parker Jr., M.G. Clerici, Appl. Catal. A 124 (1995) 107.
[24] W. Adam, I. Casades, V. Fornés, H. García, O. Weichold, J. Org. Chem. 65 (2000) 3947.
[25] C. Pazè, B. Sazak, A. Zecchina, J. Dwyer, J. Phys. Chem. B 103 (1999) 9978.
[26] S. Yang, J.N. Kondo, K. Domen, Catal. Today 73 (2002) 113.
[27] S. Bertarione, F. Bonino, F. Cesano. A. Damin, D. Scarano, A. Zecchina, J. Phys. Chem. B 112 (2008) 2580.
[28] K.B. Fogash, Z. Hong, J.M. Kobe, J.A. Dumesic, Appl. Catal. A 172 (1998) 107.
[29] K.B. Fogash, Z. Hong, J.A. Dumesic, J. Catal. 173 (1998) 519.
[30] C.H. Bartholomew, Appl. Catal. A 212 (2001) 17.
[31] D.J. Parillo, R.J. Gorte, J. Phys. Chem. 97 (1993) 8786.
[32] T. Demuth, J. Hafner, L. Benco, H. Toulhoat, J. Phys. Chem. B 104 (2000) 4593.
[33] H.P. Leftin, M.C. Hobson, Adv. Catal. 14 (1963) 115.
[34] C. Bearez, F. Chevalier, M. Guisnet, React. Kinet. Catal. Lett. 22 (1983) 405.
[35] R.A. Asuquo, G. Eder-Mirth, J.A. Lercher, J. Catal. 155 (1995) 376.
[36] R.A. Asuquo, G. Eder-Mirth, K. Seshan, J.A.Z. Pieterse, J.A. Lercher, J. Catal. 168 (1997) 292.
[37] J. Engelhardt, J. Catal. 164 (1996) 449.
[38] H.W. Kouwenhoven, W.C. van Zijll Langhout, Chem. Eng. Prog. 67 (1971) 65.

[39] N. Essayem, Y. Ben Taârit, C. Feche, P.Y. Gayraud, G. Sapaly, C. Naccache, J. Catal. 219 (2003) 97.
[40] P. Fejes, H. Förster, I. Kiricsi, J. Seebode, in: Studies in Surface Science and Catalysis – Structure and Reactivity of Modified Zeolites, vol. 18, Elsevier B.V., 1985, p. 91-98.
[41] H. Förster, S. Franke, J. Seebode, J. Chem. Soc. Faraday Trans. I 79 (1983) 373.
[42] E. Garbowski, J. Chem. Soc. Faraday Trans. I 81 (1985) 497.
[43] H. Förster, J. Seebode, P. Fejes, I. Kiricsi, J. Chem. Soc. Faraday Trans. I 83 (1987) 1109.
[44] H. Knözinger, Top. Catal. 6 (1998) 107.
[45] T.S. Sorensen, J. Am. Chem. Soc. 87 (1965) 5075.
[46] N.C. Deno, J. Bollinger, N. Friedman, K. Hafer, J.D. Hodge, J.J. Houser, J. Am. Chem. Soc. 85 (1963) 2998.
[47] N.C. Deno, in G.A. Olah, P.v.R. Schleyer (Eds.), Carbonium Ions, Wiley Interscience, New York, 1968, vol. 1.
[48] L.G. Wade, Jr., Organic Chemistry, 6th Ed., Pearson Prentice-Hall, Upper Saddle River, NJ, 2006.
[49] J. Coates, in R.A. Meyers (Ed.), Encyclopedia of Analytical Chemistry, John Wiley & Sons Ltd, Chichester, 2000.
[50] E.R. Lippincott, T.E. Kenney, J. Am. Chem. Soc. 84 (1962) 3641.
[51] L.W. Pickett, E. Paddock, E. Sackter, J. Am. Chem. Soc. 63 (1941) 1073.
[52] H.S. Cerqueira, P. Ayrault, J. Datka, M. Guisnet, Microporous Mesoporous Mater. 38 (2000) 197.
[53] T.S. Sorensen, J. Am. Chem. Soc. 87 (1965) 5075.
[54] A.G. Stepanov, M.V. Luzgin, S.S. Arzumanov, H. Ernst, D. Freude, J. Catal 211 (2002) 165.
[55] J.F. Haw, B.R. Richardson, I.S. Oshiro, N.D. Lazo, J.A. Speed, J. Am. Chem. Soc. 111 (1989) 2052.
[56] J.F. Haw, J.B. Nicholas, W. Song, F. Deng, Z. Wang, T. Xu, C.S. Heneghan, J. Am. Chem. Soc. 122 (2000) 4763.
[57] J.B. Nicholas, J.F. Haw, J. Am. Chem. Soc. 120 (1998) 11804.
[58] H. Fang, A. Zheng, J. Xu, S. Li, Y. Chu, L. Chen, F. Deng, J. Phys. Chem. C 115 (2011) 7429.
[59] E.P.L. Hunter, S.G. Lias, J. Phys. Chem. Ref. Data 27 (1998) 413.
[60] B. Arstad, S. Kolboe, Catal. Lett. 71 (2001) 209.
[61] M. Bjørgen, S. Svelle, F. Joensen, J. Nerlov, S. Kolboe, F. Bonino, L. Palumbo, S. Bordiga, U. Olsbye, J. Catal. 249 (2007) 195.
[62] S. Svelle, U. Olsbye, F. Joensen, M. Bjørgen, J. Phys. Chem. C 111 (2007) 17981.
[63] J.F. Haw, J.B. Nicholas, W.G. Song, F. Deng, Z. Wang, T. Xu, C.S. Heneghan, J. Am. Chem. Soc. 122 (2000) 4763.
[64] W. Song, J.B. Nicholas, J.F. Haw, J. Phys. Chem. B 105 (2001) 4317.
[65] D.M. McCann, D. Lesthaeghe, P.W. Kletnieks, D.R. Guenther, J.J. Hayman, V. Van Speybroeck, M. Waroquier, J.F. Haw, Angew. Chem., Int. Ed. 47 (2008) 5179.
[66] J.-P. Lange, A. Gutsze, J. Allgeier, H.G. Karge, Appl. Catal. 45 (1988) 345.
[67] R.A. Friedel, M. Orchin, Ultraviolet Spectra of Aromatic Compounds, Wiley, New York, 1951.
[68] R.N. Jones, Chem. Rev. 41 (1947) 353.

[69] R.A. Friedel, M.A. Orchin, Ultraviolet spectra of aromatic compounds, John Wiley & Sons, New York, 1951, p. 532.
[70] S.M. Leschev, A.V. Sin'kevich, Russ. J. Appl. Chem. 76 (2003) 1483.
[71] W.K Hall, J. Catal. 1 (1962) 53.
[72] L.S. Singer, I.C. Lewis, J. Am. Chem. Soc. 87 (1965) 4695.
[73] H.-H. Perkampus, E. Baumgarten, Angew. Chem., Int. Ed. 3 (1964) 776.
[74] G. Dallinga, E.L. Mackor, A.A.V. Stuart, Mol. Phys. 1 (1958) 123.

Figures

Fig. 1

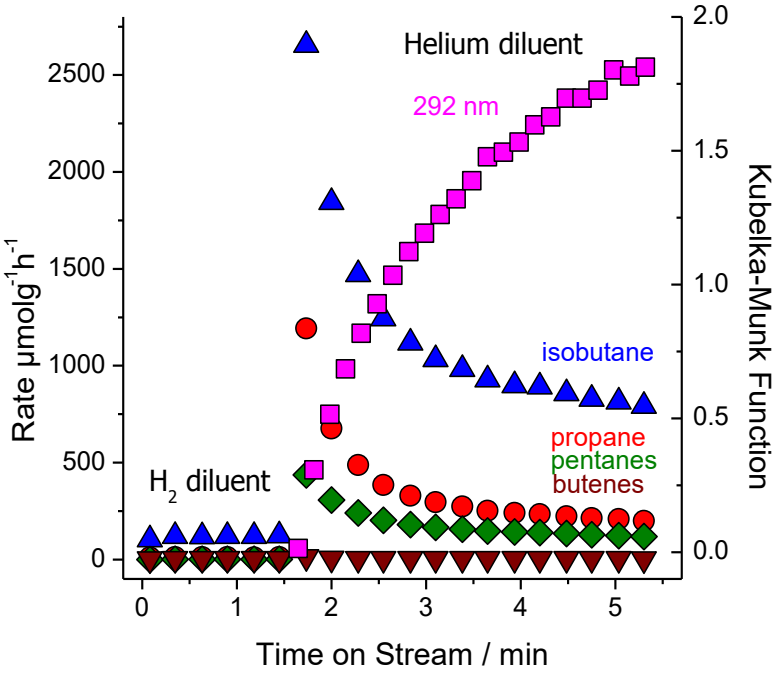

Fig. 1: Rates of formation of gas phase products during conversion of *n*-butane (10 kPa partial pressure) on H-mordenite (M1, W/F = 0.16 h) at a reaction temperature 563 K using either H_2 (first 1.5 h) or helium (after 1.5 h) as the diluent. The Kubelka-Munk value at 292 nm is plotted on the right axis. The corresponding UV–vis spectra are shown in Fig. 2.

Fig. 2

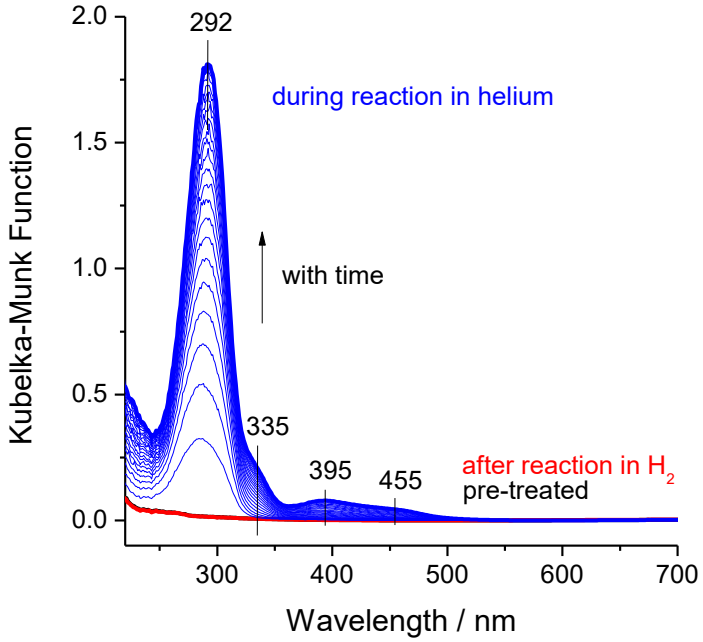

Fig. 2: Evolution of diffuse reflectance UV–vis spectra recorded in situ during conversion of *n*-butane (10 kPa partial pressure) on H-mordenite (M1, W/F = 0.16 h) at a reaction temperature of 563 K. The corresponding gas phase products are shown in Fig. 1. Black line: pre-treated catalyst; red line (superimposed on black line): last spectrum in *n*-butane/H_2; blue lines: in *n*-butane/helium.

Fig. 3

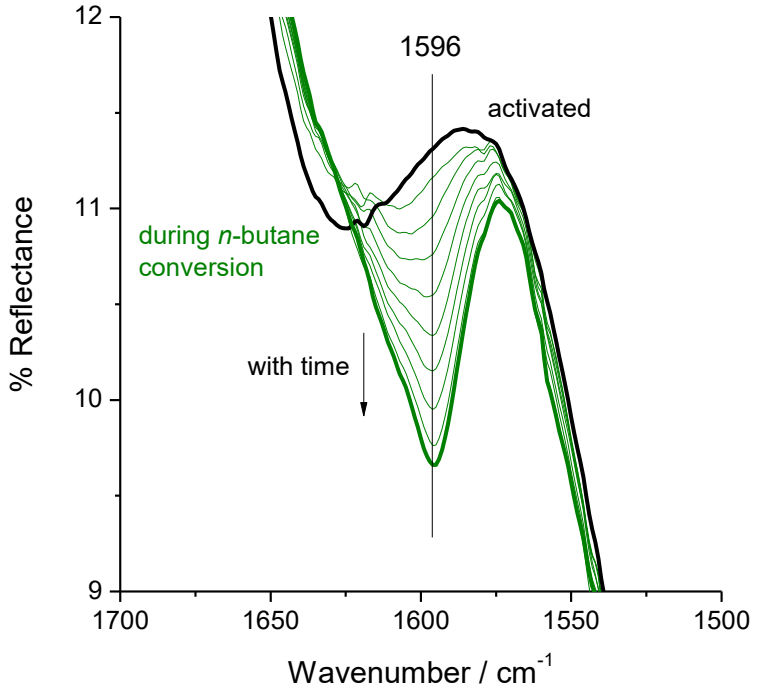

Fig. 3: Evolution of diffuse reflectance infrared spectra recorded in situ during conversion of *n*-butane (10 kPa partial pressure) on H-mordenite (M1, W/F = 0.13 h) at a reaction temperature of 633 K using helium as the diluent. Black line: pre-treated catalyst; green lines: during conversion of *n*-butane. The time interval between spectra is 20 minutes. The resolution is 4 cm^{-1}.

Fig. 4

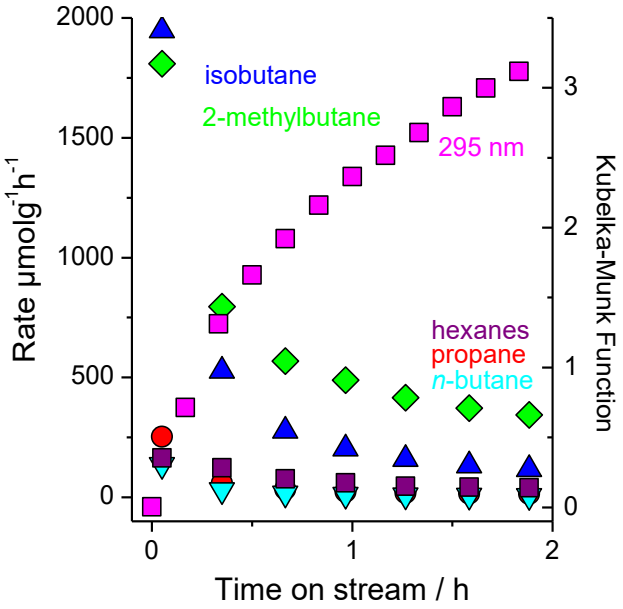

Fig. 4: Rates of formation of gas phase products during conversion of *n*-pentane (13 kPa partial pressure) on H-mordenite (M1, W/F = 0.08 h) at 453 K using helium as the diluent. The Kubelka-Munk value at 295 nm is plotted on the right axis. The corresponding UV–vis spectra are shown in Fig. 5.

Fig. 5

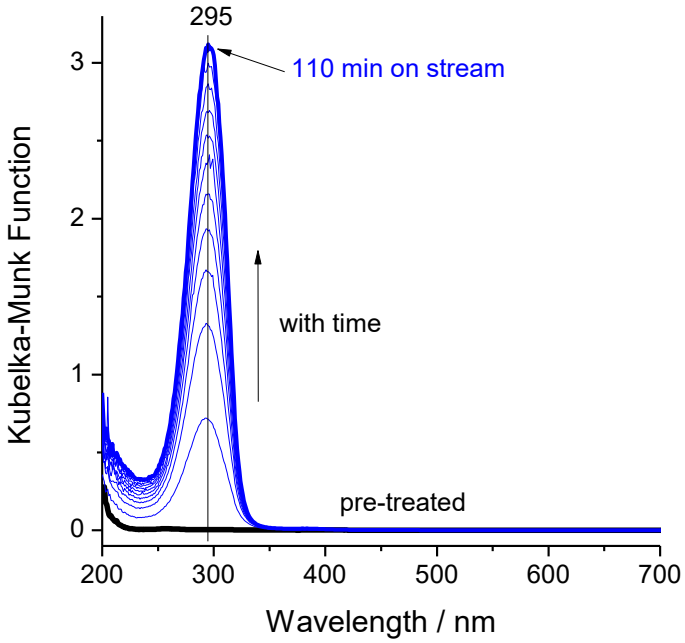

Fig. 5: Evolution of diffuse reflectance UV–vis spectra recorded in situ during conversion of *n*-pentane (13 kPa partial pressure) on H-mordenite (M1, W/F = 0.08 h) at a reaction temperature of 453 K using helium as the diluent. Black line: pre-treated catalyst; blue lines: in *n*-pentane/helium.

Fig. 6

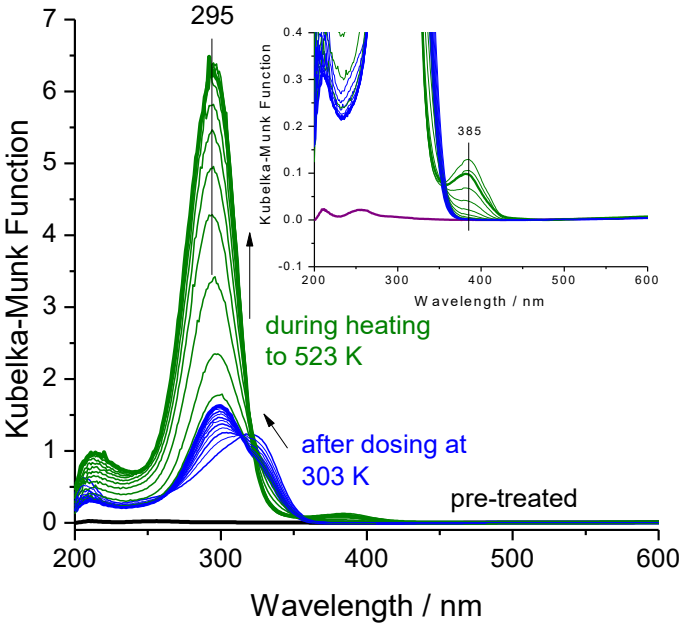

Fig. 6: Diffuse reflectance UV–vis spectra of H-mordenite (M1) recorded in situ during exposure to 1-pentene at a temperature of 303 K. Five µL of 1-pentene vapor was taken from the headspace above 1-pentene liquid and then injected. The in situ cell was held at 303 K for 2 h (blue lines) and then heated at 2 K min^{-1} to 523 K (green lines). Spectra were collected in 10 minute intervals. Pre-treatment was at 673 K in N_2.

Fig. 7

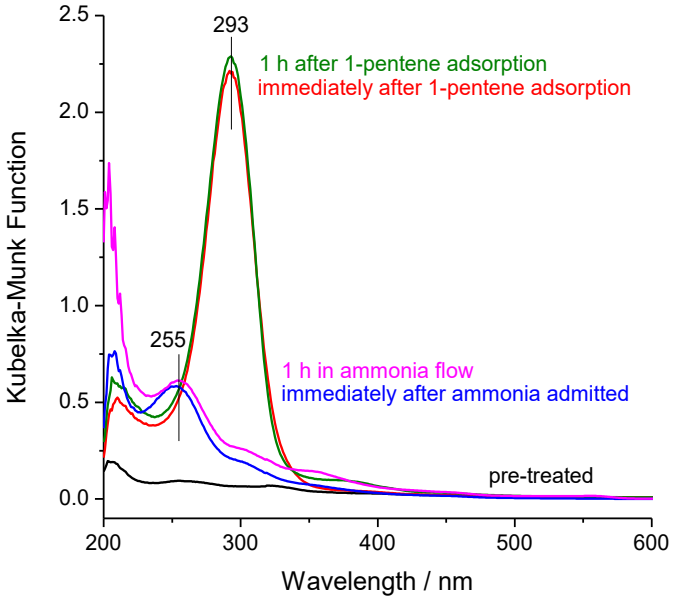

Fig. 7: Diffuse reflectance UV–vis spectra of H-mordenite (M1) recorded in situ during exposure to 1-pentene at a temperature of 453 K. Five µL of 1-pentene vapor was taken from the headspace above 1-pentene liquid and then injected. The in situ cell was held at 453 K for 2 h, the first hour in a helium flow of 30 ml min^{-1} and the second hour with 5 ml min^{-1} of a 2% ammonia in helium mixture added to the original helium flow. Pre-treatment was at 673 K in N_2.

Fig. 8

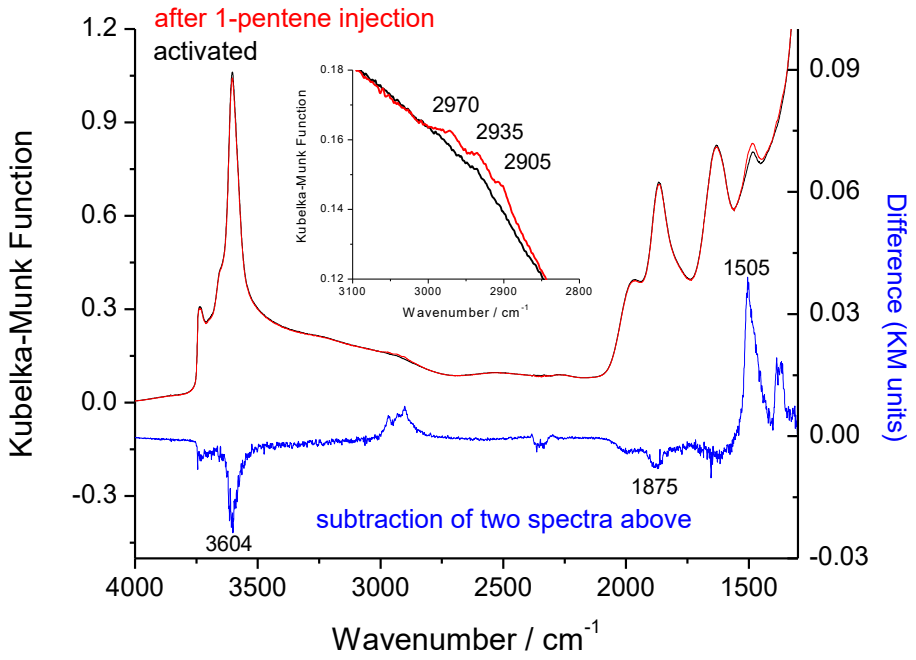

Fig. 8: Diffuse reflectance infrared spectra of a physical mixture of H-mordenite (M1) and KBr (1:2 mass ratio) recorded in situ before (pre-treated, black line) and after (red line) introduction of 0.2 µL 1-pentene (injected as liquid) with the chamber at a temperature of 453 K. The blue line is a subtraction of the black line from the red line. The resolution is 2 cm^{-1}. The zeolite was pre-treated at 573 K in N_2.

Fig. 9

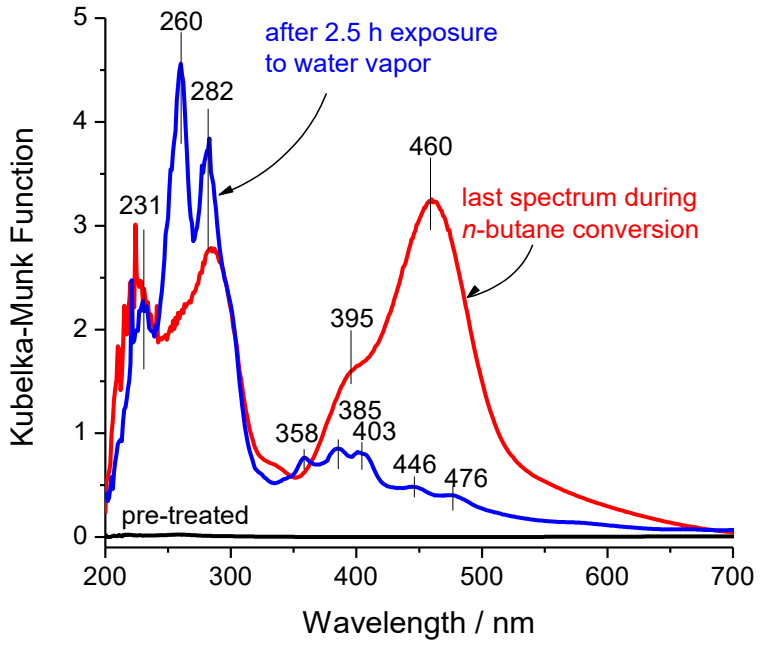

Fig. 9: Diffuse reflectance UV–vis spectra of pre-treated, spent and humidified catalyst. *n*-Butane (10 kPa partial pressure) conversion was performed on H-mordenite (M1) for 2 h at a reaction temperature of 636 K using helium as the diluent. The *n*-butane was then removed from the gas stream and the chamber was cooled to 303 K. The gas flow was then switched to 5 ml min^{-1} N_2 saturated with water vapor. Black line: pre-treated catalyst; red line: last spectrum during conversion of *n*-butane; blue line: after 2.5 h exposure to water vapor.

Fig. 10

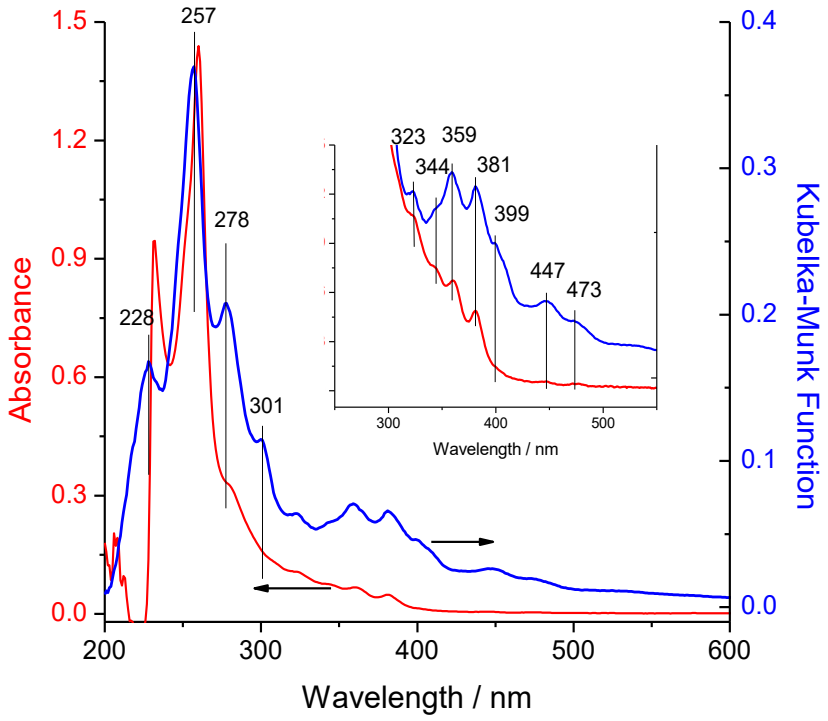

Fig. 10: UV–vis spectra of spent catalyst and extract. H-mordenite (M2) was activated in an isothermal reactor, exposed to 1-butene at a temperature of 323 K, heated to 573 K, and held for 1 h. The two spectra represent the solid, ambient-exposed H-mordenite before digestion (blue line, Kubelka–Munk scale) and the dichloromethane extract obtained after digestion (red line, absorbance scale).

Fig. 11

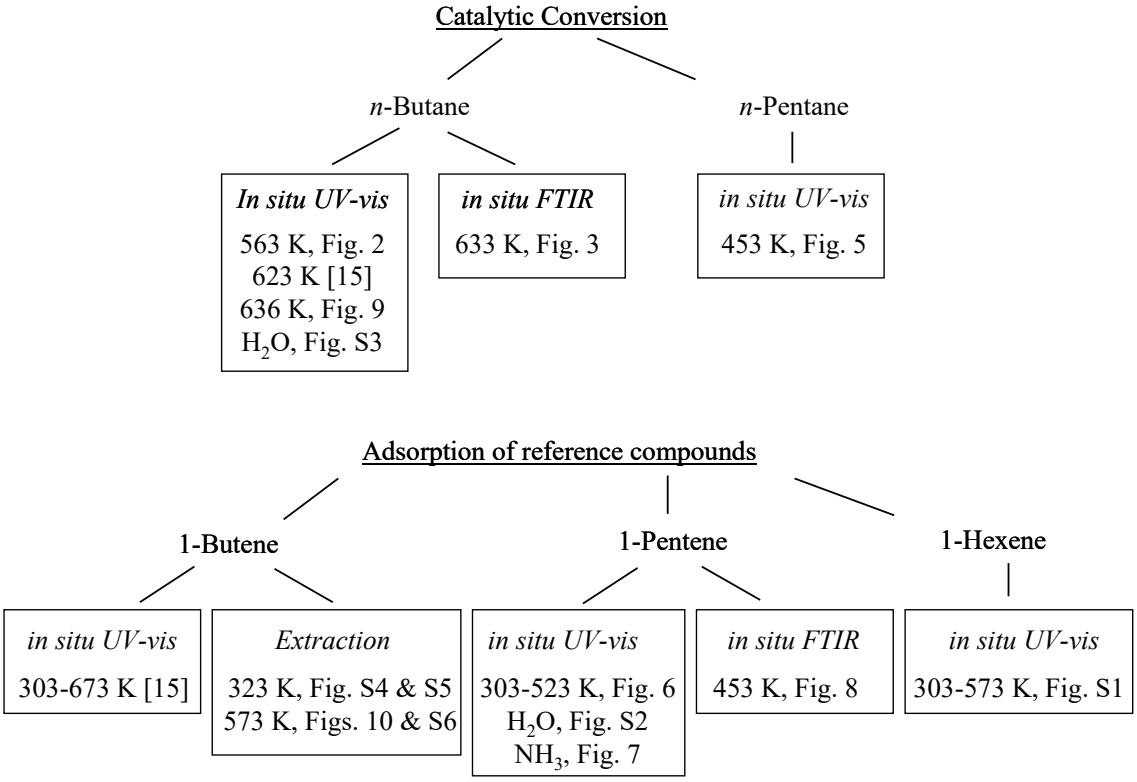

Fig. 11: Outline of reported experiments and figures.

Identification of carbonaceous deposits formed on H-mordenite during alkane isomerization

Matthew J. Wulfers and Friederike C. Jentoft

Supporting Information

Fig. S1

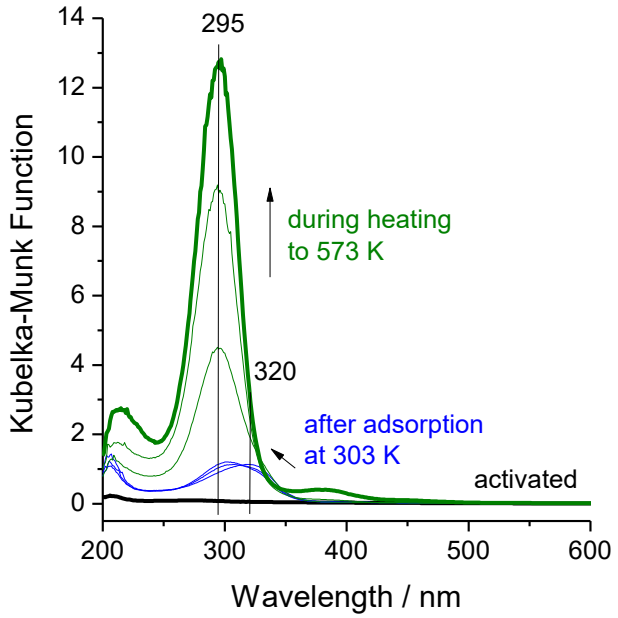

Fig. S1: Diffuse reflectance UV–vis spectra of H-mordenite (M1) recorded in situ during exposure to 1-hexene at a temperature of 303 K. 1 µL of liquid 1-hexene was injected and the cell was held at 303 K for 30 minutes (blue line) and then heated at 10 K min^{-1} to 573 K (green lines). Spectra were taken in 10 minute intervals. Pre-treatment was performed at 673 K with sequential 30 minute treatments in synthetic air, N_2, and H_2.

Fig. S2

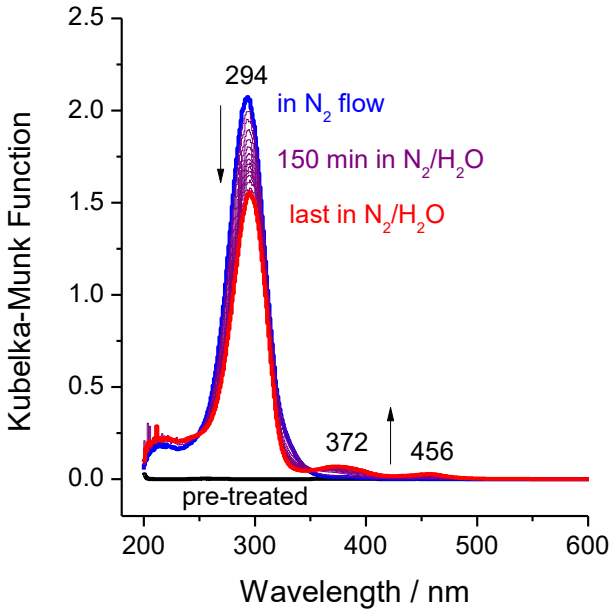

Fig. S2: Diffuse reflectance UV–vis spectra of H-mordenite (M2) recorded in situ after exposure to 0.1 µL of 1-pentene (injected as liquid) at a temperature of 373 K (blue line) and after application of water vapor at 303 K (purple lines). Spectra were taken in 10 minute intervals. Pre-treatment was performed at 673 K in 30 ml min^{-1} N_2.

Fig. S3

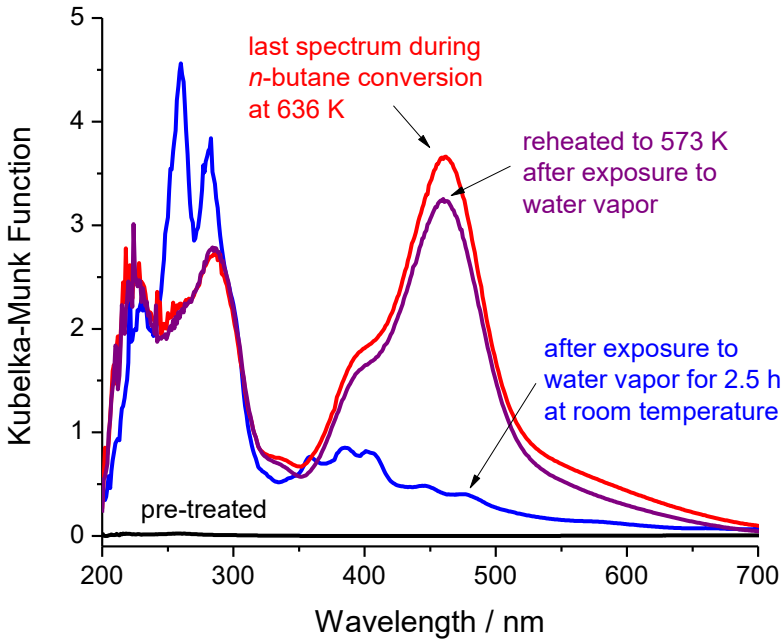

Fig. S3: Diffuse reflectance UV–vis spectra of pre-treated, spent, humidified, and re-heated catalyst. The red and blue spectra are the same shown in Fig. 9. After exposure to water vapor at a temperature of 303 K for 2.5 h, the catalyst was re-heated to 573 K in a stream of pure N_2 (purple line).

Fig. S4

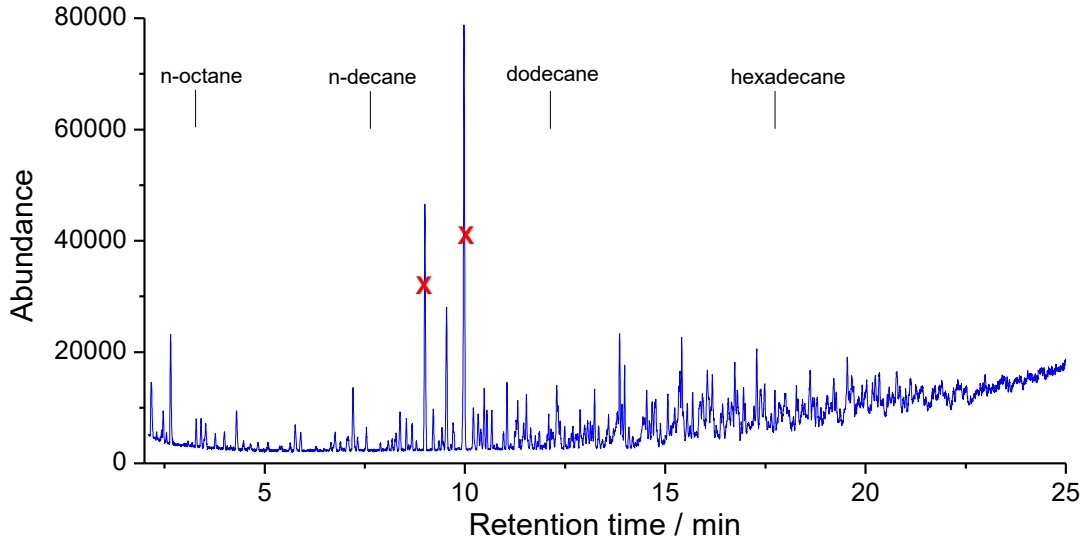

Fig. S4: GC-MS chromatogram of the dichloromethane extract collected from H-mordenite (M2) after exposure to 1-butene at a temperature of 323 K and digestion in hydrofluoric acid. The retention times of several reference compounds are provided. The UV–vis spectrum of the dichloromethane extract is shown in Fig. S5. The red X indicate known *cis*- and *trans*-decalin impurities leached from the polyethylene vials.

Fig. S5

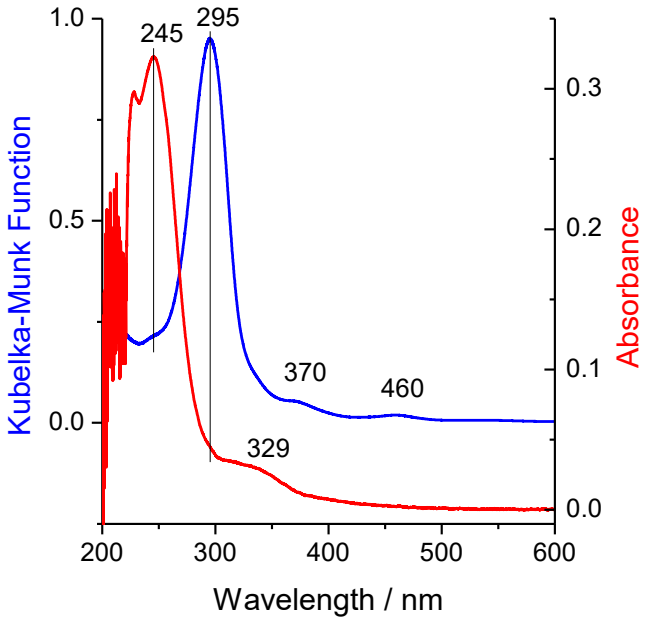

Fig. S5: Diffuse reflectance UV–vis spectrum of H-mordenite (M2) after exposure to 1-butene at a temperature 323 K and transfer under ambient conditions (blue line) and transmission UV–vis spectrum the dichloromethane extract (red line) collected after digestion of the zeolite in hydrofluoric acid. The GC-MS chromatogram of the dichloromethane extract is shown in Fig. S4.

Fig. S6

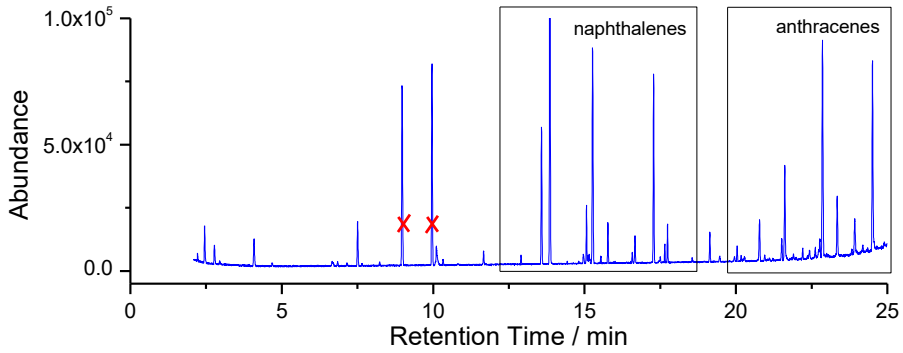

Fig. S6: GC-MS chromatogram of the dichloromethane extract collected from H-mordenite (M2) after exposure to 1-butene at a temperature of 573 K and digestion in hydrofluoric acid. The UV-vis spectrum of the dichloromethane extract is shown in Fig. 10. The red X indicate known *cis*- and *trans*- decalin impurities leached from the polyethylene vials.